Electron-proton scattering

1. Elastic ep-scattering and the proton radius
2. Deep-inelastic (DIS) electron proton scattering

(1) Is largely a recap of PEP4 (we will not discuss all details)

For reference:
This section of the lecture follows closely chapter 7 and 8 of M. Thomson's Modern Particle Physics however provide a few more recent experimental results.

Electron-proton scattering

Relativistic electron-proton scattering probe the structure of the proton:

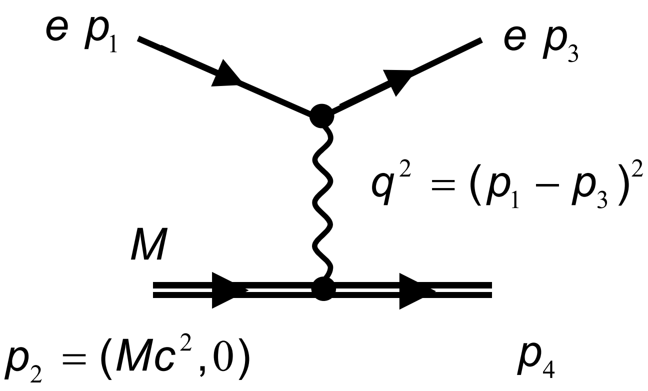

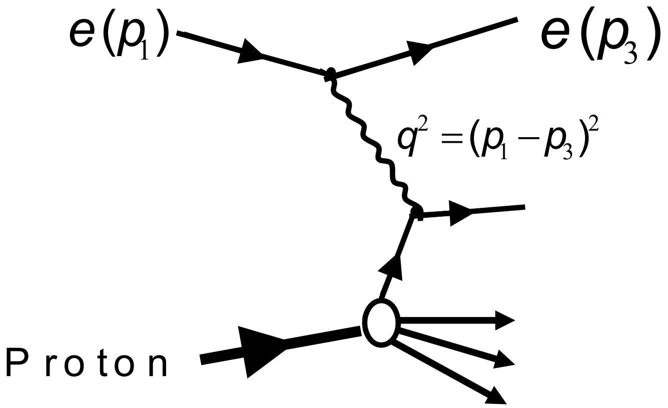

- at “low energy” - elastic scattering is dominant process: “virtual photon” probes the proton as whole and provides proton properties like the charge radius (PEP4)
- At “high energy” – inelastic scattering: proton breaks up. Understood as the elastic scattering of the electron on point-like charged proton constitutes, i.e. quarks.

Relevant quantity to distinguish between the diff. regimes is $Q^2=-q^2$ of virtual photon:

$1/Q^2 >> r_p^2$: proton appears point like (Rutherford)
$1/Q^2 \approx r_p^2$: proton charge distribution resolved (Rosenbluth)
$1/Q^2 << r_p^2$: probe internal proton structure (DIS)

1. Elastic ep-scattering and the proton radius

In the limit that the proton can be treated as a point-like spin ½ particle (Dirac fermion, ignore inner degrees of freedom) one can use QED Feynman rules to write down the matrix element (assume highly relativistic electrons $E_1 >> m_e$):

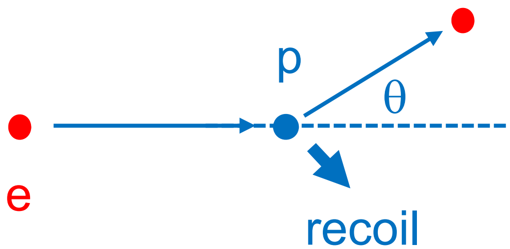

In general only electron quantities measured.

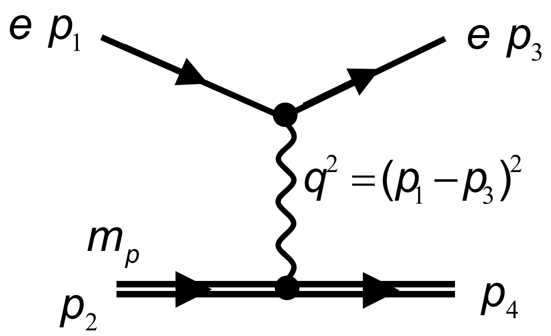

$$p_1 = (E_1, 0, 0, E_1)$$
$$p_2 = (m_p, 0, 0, 0)$$
$$p_3 = (E_3, 0, E_3 \sin\theta, E_3 \cos\theta)$$
$$p_4 = (E_4, \vec{p}_4)$$

If one ignores p recoil: $q^2 = (0, \vec{p}_1 - \vec{p}_3)^2 = \vec{q}^{\,2}$

$$\mathcal{M}_{fi} = \frac{e^2}{q^2}\left[\bar{u}(p_3)\gamma_\mu u(p_1)\right]\left[\bar{u}(p_4)\gamma^\mu u(p_2)\right]$$

Following the prescription of the QED theory lecture one can determine the average matrix element summed over all final state spin states:

$$\left\langle |\mathcal{M}|^2 \right\rangle = \frac{8e^4}{q^4}\left[(p_1p_2)(p_3p_4) + (p_1p_4)(p_2p_3) - m_p^2(p_1p_3)\right]$$

$$= (p_2p_4)$$

Using $Q^2 = -q^2 = -(p_1 - p_3)^2 = \ldots = 4E_1E_3\sin^2\left(\frac{\theta}{2}\right)$

$$(1-\cos\theta) = 2\sin^2\frac{\theta}{2}$$

with $\left\{ \begin{array}{l} p_4 = p_2 + p_1 - p_3 \\ p_1^2 = p_3^2 = m_e^2 \approx 0 \qquad p_2^2 = p_4^2 = m_p^2 \end{array} \right.$

One finds: $\left\langle |\mathcal{M}|^2 \right\rangle = \frac{m_p^2 e^4}{E_1 E_3 \sin^2\left(\frac{\theta}{2}\right)}\left[\cos^2\left(\frac{\theta}{2}\right) + \frac{Q^2}{2m_p^2}\sin^2\left(\frac{\theta}{2}\right)\right]$

Resulting in the differential cross section in the lab:

$$\boxed{\frac{d\sigma}{d\Omega} = \frac{\alpha^2}{4E_1^2\sin^4\left(\frac{\theta}{2}\right)}\cdot\left(\frac{E_3}{E_1}\right)\left[\cos^2\left(\frac{\theta}{2}\right) + \frac{Q^2}{2m_p^2}\sin^2\left(\frac{\theta}{2}\right)\right]}$$

Often called “Dirac cross section“:
e-scattering at a “point-like” proton (academic case!)

Reminder in CMS:

$$\frac{d\sigma}{d\Omega_f} = \frac{1}{64\pi^2 s}\frac{p_f}{p_i}|\mathcal{M}_{fi}|^2$$

In lab for fixed target:

$$\frac{\mathrm{d}\sigma}{\mathrm{d}\Omega} \approx \frac{1}{64\pi^2}\left(\frac{E_3}{m_\mathrm{p}E_1}\right)^2\langle|\mathcal{M}_{fi}|^2\rangle$$

(See e.g. Thomson, Ch 3)

$$\boxed{\frac{d\sigma}{d\Omega} = \frac{\alpha^2}{4E_1^2 \sin^4\left(\frac{\theta}{2}\right)} \cdot \left(\frac{E_3}{E_1}\right)\left[\cos^2\left(\frac{\theta}{2}\right) + \frac{Q^2}{2m_p^2}\sin^2\left(\frac{\theta}{2}\right)\right]}$$

We can recognize different well known pieces:

- Rutherford cross section for scattering of a scalar particle on a Coulomb potential:

$$\left.\frac{d\sigma}{d\Omega}\right|_{\text{`}Rutherf} = \frac{\alpha^2}{4E_1^2 \sin^4\left(\frac{\theta}{2}\right)}$$

- Term E_3/E_1 accounts for the electrons energy loss due to the proton recoil.

- Mott cross section: for relativistic electron scattering w/ spin ½ at a Coulomb potential of a point-like particle in the limit $Q^2 << m_p^2$ and $E_1 < m_p$ (see PEP4):

$$\left.\frac{d\sigma}{d\Omega}\right|_{\text{`}Mott} = \frac{\alpha^2}{4E_1^2 \sin^4\left(\frac{\theta}{2}\right)} \cdot \left(\frac{E_3}{E_1}\right)\cos^2\left(\frac{\theta}{2}\right)$$

Term $\sim \frac{Q^2}{2m_p^2}\sin^2\left(\frac{\theta}{2}\right)$ describes the magnetic interaction between the spin of the electron and the proton spin (relevant only for large Q^2)

In case of electron scattering at an extended charge distribution the Mott cross section needs to be corrected by the form factor of the charge distribution:

$$\frac{d\sigma}{d\Omega} = \left.\frac{d\sigma}{d\Omega}\right|_{`Mott} \cdot \left|F(\vec{q})\right|^2$$ (discussed in PEP4)

With the form factor being the Fourier transform of the charge distribution:

$$F(\vec{q}) = \int \rho(\vec{r}) e^{i\vec{q}\vec{r}} d\vec{r}$$

$$= F(\vec{q}^{\,2})$$ for spherical symmetric charge distributions $\rho(r)$ (integration over the polar angle possible) → F is a function of q^2

For $\vec{q}\vec{r} \ll \hbar$ one can expand the integrand and obtains:

$$F(\vec{q}^{\,2}) = 1 - \frac{1}{6}\vec{q}^{\,2}\left\langle r^2 \right\rangle + \ldots$$ where $\left\langle r^2 \right\rangle = \int r^2 \rho(r) d^3 r$ is the mean quadratic charge radius

$\left\langle r^2 \right\rangle$ can thus be determined from the gradient of the form factor $F(\vec{q}^{\,2})$ at $\vec{q}^{\,2} \to 0$

$$\left\langle r^2 \right\rangle = -6 \left.\frac{dF(\vec{q}^{\,2})}{d\vec{q}^{\,2}}\right|_{\vec{q}^{\,2}=0}$$ formula used to extract the proton charge radius $\left\langle r_p^2 \right\rangle$ (see below)

Form factors for different charge distributions:

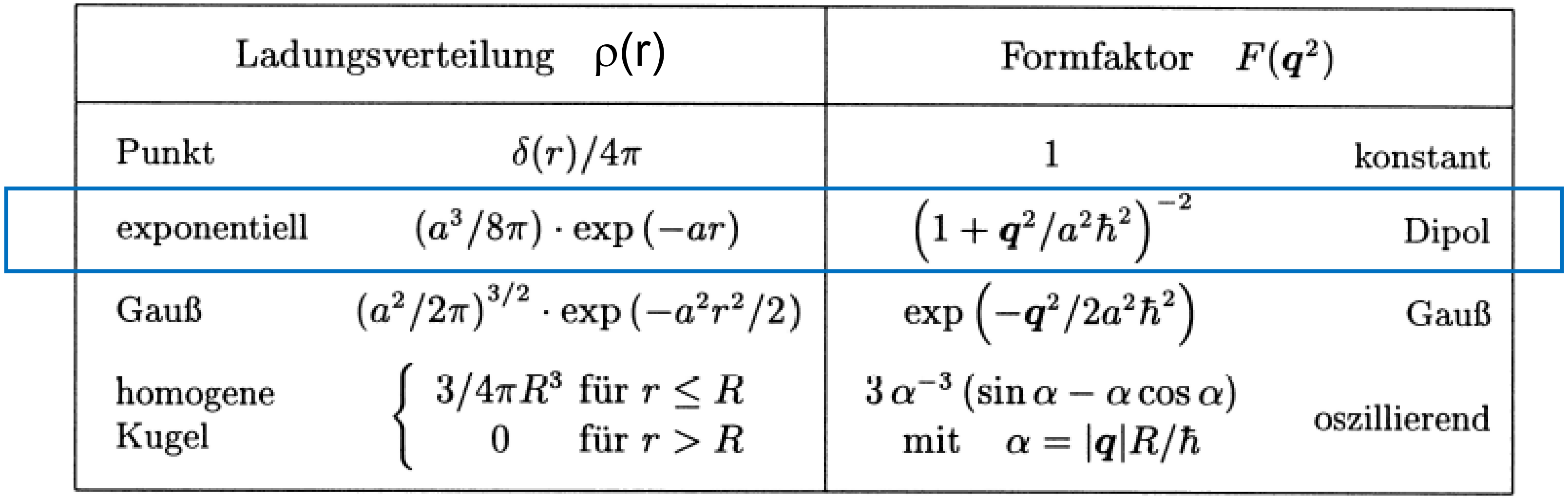

Ladungsverteilung $\rho(r)$		Formfaktor $F(\boldsymbol{q}^2)$	
Punkt	$\delta(r)/4\pi$	1	konstant
exponentiell	$(a^3/8\pi)\cdot\exp(-ar)$	$\left(1+\boldsymbol{q}^2/a^2\hbar^2\right)^{-2}$	Dipol
Gauß	$(a^2/2\pi)^{3/2}\cdot\exp(-a^2r^2/2)$	$\exp\left(-\boldsymbol{q}^2/2a^2\hbar^2\right)$	Gauß
homogene Kugel	$\begin{cases} 3/4\pi R^3 & \text{für } r\le R \\ 0 & \text{für } r>R \end{cases}$	$3\,\alpha^{-3}\,(\sin\alpha-\alpha\cos\alpha)$ mit $\alpha=\lvert\boldsymbol{q}\rvert R/\hbar$	oszillierend

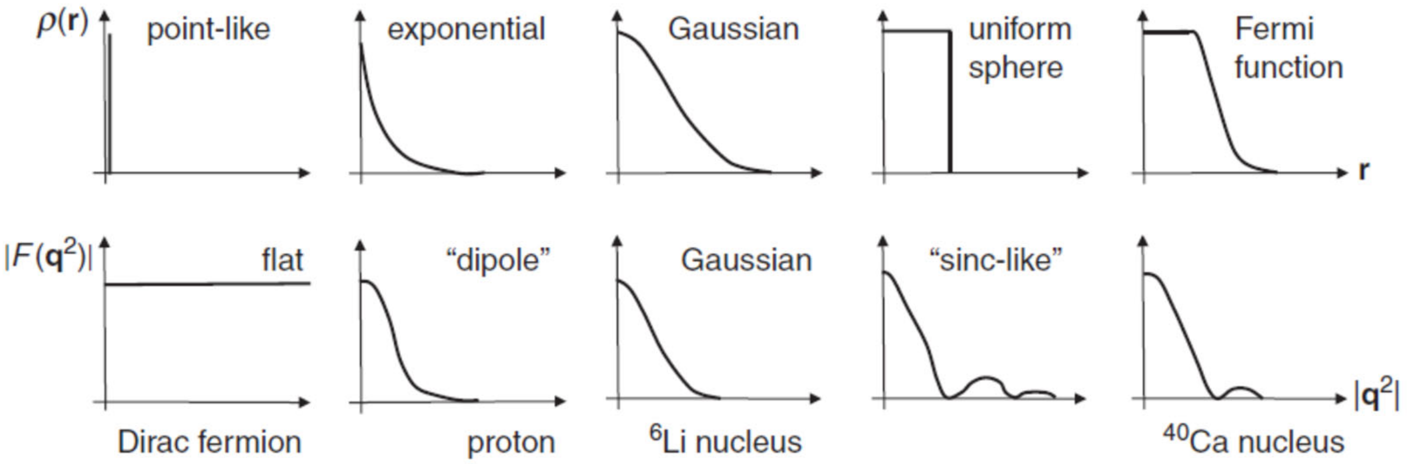

Possible three-dimensional charge distributions and the corresponding form factors plotted as a function of $\mathbf{q}^2$.

(from Thomson, Modern Particle Physics)

e - scattering on an extended proton

Following the introduction of the form factors for Mott scattering two form-factors are introduced to account for the finite size of the proton in the Dirac formula:

$G_E(Q^2)$ related to the charge distribution $\rho(r)$

$G_M(Q^2)$ related to the magnetic moment distribution $\mu(r)$

The elastic electron-proton cross section can be written as;

$$\frac{d\sigma}{d\Omega} = \frac{\alpha^2}{4E_1^2 \sin^4\left(\frac{\theta}{2}\right)} \cdot \left(\frac{E_3}{E_1}\right)\left[\frac{G_E^2 + \tau G_M^2}{1+\tau}\cos^2\left(\frac{\theta}{2}\right) + 2\tau G_M^2 \sin^2\left(\frac{\theta}{2}\right)\right] \quad \text{w/} \quad \tau = \frac{Q^2}{4m_p^2}$$

Remarks:

Form factors depend on the Q^2 = 4-vector of the virtual photon (FF in the elastic Mott cross section were dependent on 3-vector $\vec{q}$) and therefore cannot be simply interpreted as the Fourier transform of the charge / magnetic moment distribution.

However in the limit $Q^2 << m_p^2$ ($Q^2 \approx \vec{q}^2$) the Fourier transform is recovered:

$$G_E(Q^2) \approx G_E(\vec{q}^2) \approx \int \rho(r)\, e^{i\vec{q}\vec{r}}\, d\vec{r}$$

$$G_M(Q^2) \approx G_M(\vec{q}^2) \approx \int \mu(r)\, e^{i\vec{q}\vec{r}}\, d\vec{r}$$

Rosenbluth / Dirac cross section was obtained for a Dirac fermion with g=2:

$$\vec{\mu} = 2 \cdot \frac{q}{2m} \vec{S}$$

The proton however is a composed object and experimentally the g-factor is

$$g_p = +5.58 \qquad \vec{\mu} = 2.79 \cdot 2 \cdot \frac{q}{2m} \vec{S}$$

To correctly describe the experimental observation the magnetic moment distribution has to be normalized correspondingly:

$$G_E(0) \approx \int \rho(r)\, e^{i\vec{q}\vec{r}}\, d\vec{r} = 1$$

$$G_M(0) \approx \int \mu(r)\, e^{i\vec{q}\vec{r}}\, d\vec{r} = 2.79$$

i.e., if one assumes the same shape for G_E and G_M, one expects G_M to be scaled up by a factor 2.79.

Determination of $G_E(Q^2)$ and $G_M(Q^2)$

Although one expects similar shape for the two form factors, G_E and G_M should be determined independently. Dividing the Rosenbluth formula by the Mott cross section one obtains:

$$\frac{d\sigma}{d\Omega}\Big/\left.\frac{d\sigma}{d\Omega}\right|_{\text{`}Mott} = \left[\frac{G_E^2(Q^2)+\tau G_M^2(Q^2)}{1+\tau} + 2\tau G_M^2(Q^2)\tan^2\left(\frac{\theta}{2}\right)\right] = A(Q^2) + B(Q^2)\tan^2\left(\frac{\theta}{2}\right)$$

with $\tau = Q^2 / 4m_p^2$

While low Q^2 data determines $G_E^2(Q^2)$ and high Q^2 data determines $G_M^2(Q^2)$ one can obtain $G_E^2(Q^2)$ and $G_M^2(Q^2)$ for general Q^2 using the **Rosenbluth separation**

Cross section is measured for different electron energy E_1 and different scattering angle θ → plot the Mott normalized cross section as function of $\tan\theta/2$

Rosenbluth separation

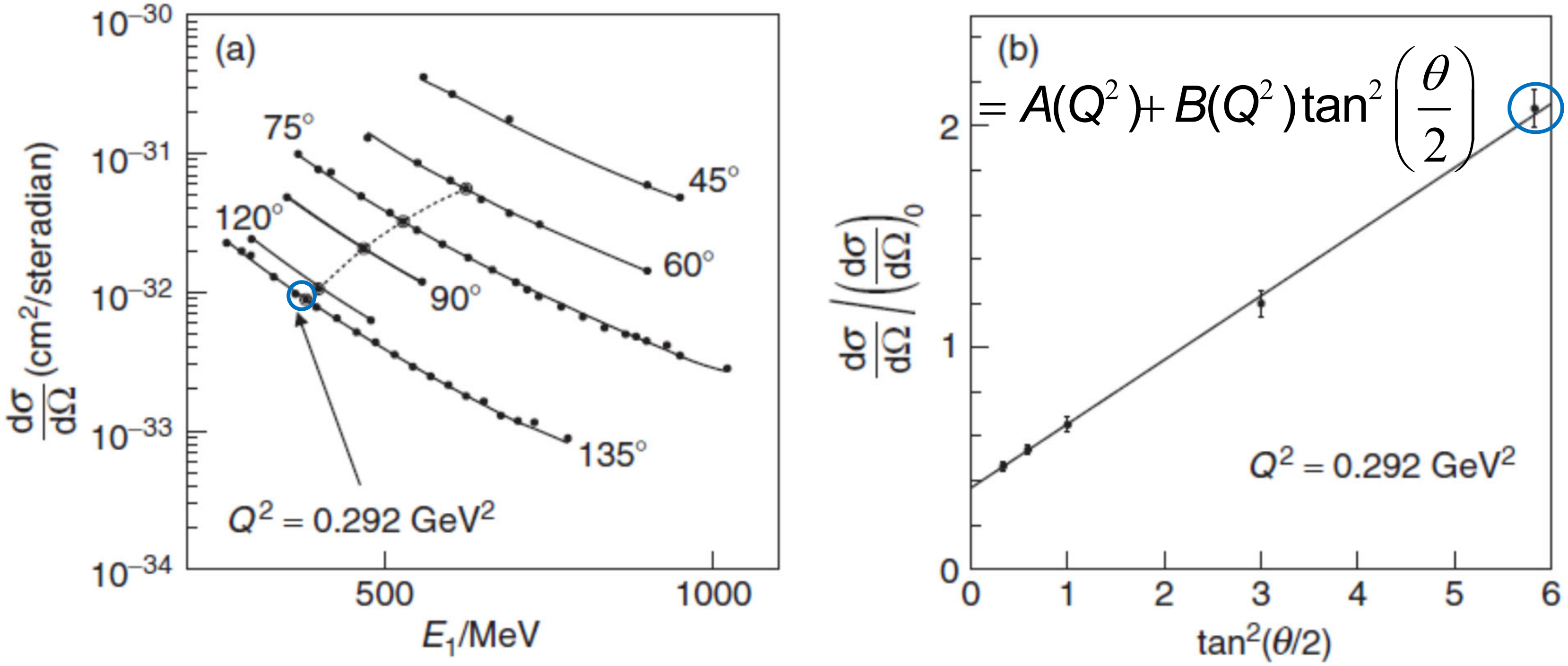

$$= A(Q^2) + B(Q^2)\tan^2\left(\frac{\theta}{2}\right)$$

(from Thomson, Modern Particle Physics)

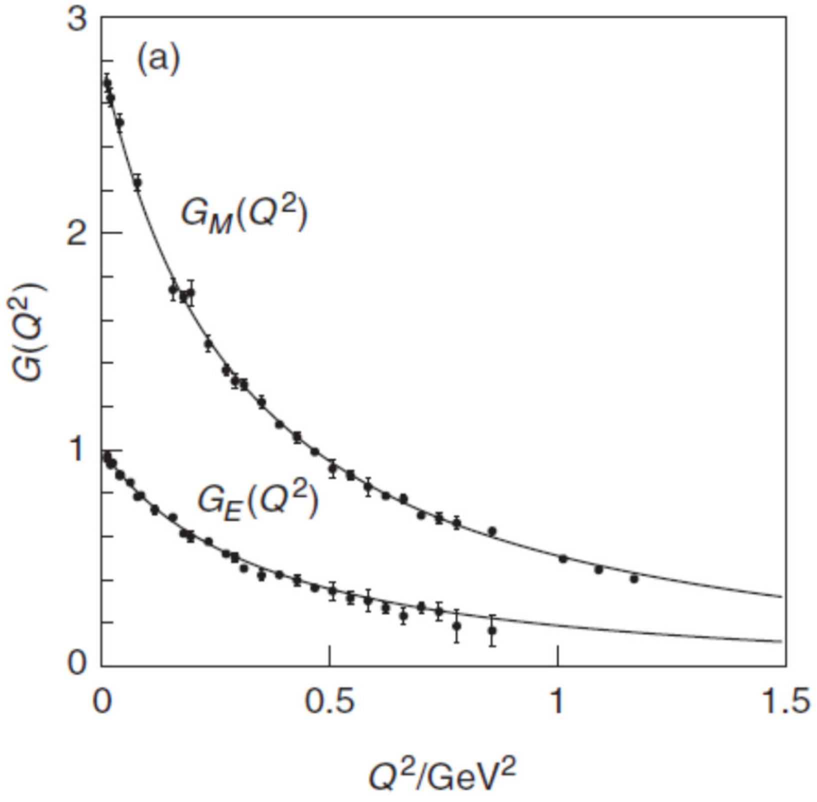

Taken from Thomson,
Data from E. B. Hughes et al. (1965)

The solid line is a dipole form factor model:

$$G(Q^2) = \left(1 + \frac{Q^2}{0.71\,\mathrm{GeV}^2}\right)^{-2}$$

= form factor of exponential charge distr.

$$\rho(r) = e^{-ar} \quad \text{with} \quad a=4.27\ \mathrm{fm}^{-1}$$

$$0.71\mathrm{GeV}^2 = a^2\hbar^2 \rightarrow a = 4.27\mathrm{fm}^{-1}$$

One also finds that G_E and G_M follow the same dipole shape (but scaled by 2.79).

From the exponential distribution one can determine the proton charge radius, defined as $\langle r^2 \rangle^{1/2}$ one finds r_p = 0.81 fm.

Instead of fitting the form factor shape one can also extrapolate to $Q^2 = 0$ an determine the slope at $Q^2 = 0$ of the measured behavior (see above)

$$\langle r^2 \rangle = -6\left[\frac{dG(Q^2)}{dQ^2}\right]_{Q^2=0}$$

done in many recent measurements.

Most precise determination of the proton charge radius from ep scattering:

A1 collaboration at Mainz Microtron (MAMI):

electron beams of 150 – 855 MeV, liquid hydrogen target and 3 high resolution spectrometers
Variation of scattering angles and beam energy in more than 500 settings (J.C. Bernauer et al. PRL 105 (2010) 242001 and PRC 90 (2014) 015206)

https://arxiv.org/pdf/1307.6227

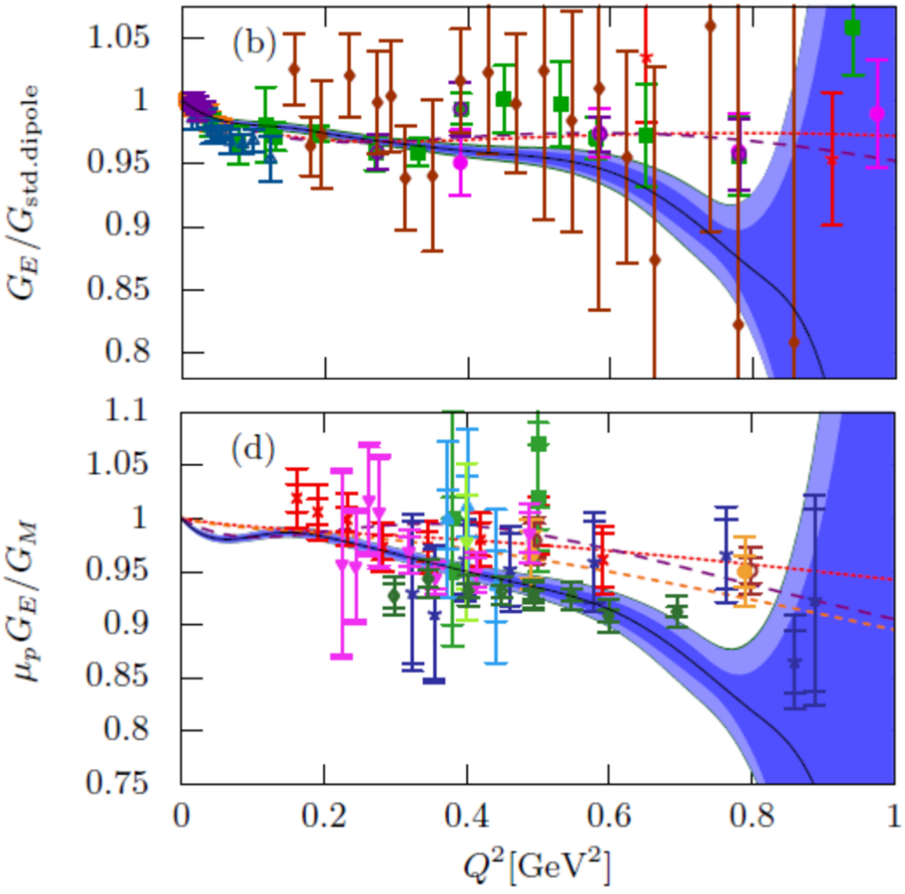

Authors determine a proton electric charge radius of

$$r_p = 0.879(7)\,\text{fm}$$

Consistent with earlier ep scattering Results but inconsistent with the most recent results from spectroscopy.

Proton radius from Lamb shift determined in hydrogen spectroscopy

2s-2p transition frequency (Lamb shift) is influenced by the overlap of the 2s orbital with H^+ (proton) charge distribution (p-orbitals have no overlap).

Sensitivity to the proton radius is low (difficult to make precise measurement):

$$\Delta E^{FS}_{ns-np} \sim \frac{(Z\alpha)^4}{3n^3} \cdot \underset{\substack{\uparrow \\ \text{reduced mass}}}{m_r^3} \cdot \langle r_p^2 \rangle$$

However w/ muonic hydrogen w/ $m_\mu \approx 200\ m_e$ the effect is about 10^7 times larger: Measurement of 2s-2p splitting in muonic hydrogen allows precise determination of the proton charge radius $r_{p.}$

<u>Muonic-hydrogen (μp) experiment at PSI:</u>

μ^- stopped in a hydrogen target → highly excited μp atoms (n≈14):
The excited atoms mostly de-excite to the 1s ground state.
About 1% of de-excitation also populate the stable 2s state.

Using laser light (~6μm) to induce the 2s-2p transition
→ de-excitation to 1s ground state → emission of 1.9 keV X-ray

Method: measure the emission of X-rays as a function of the laser tuning.

R. Pohl et al, Nature 466 (2010) 213

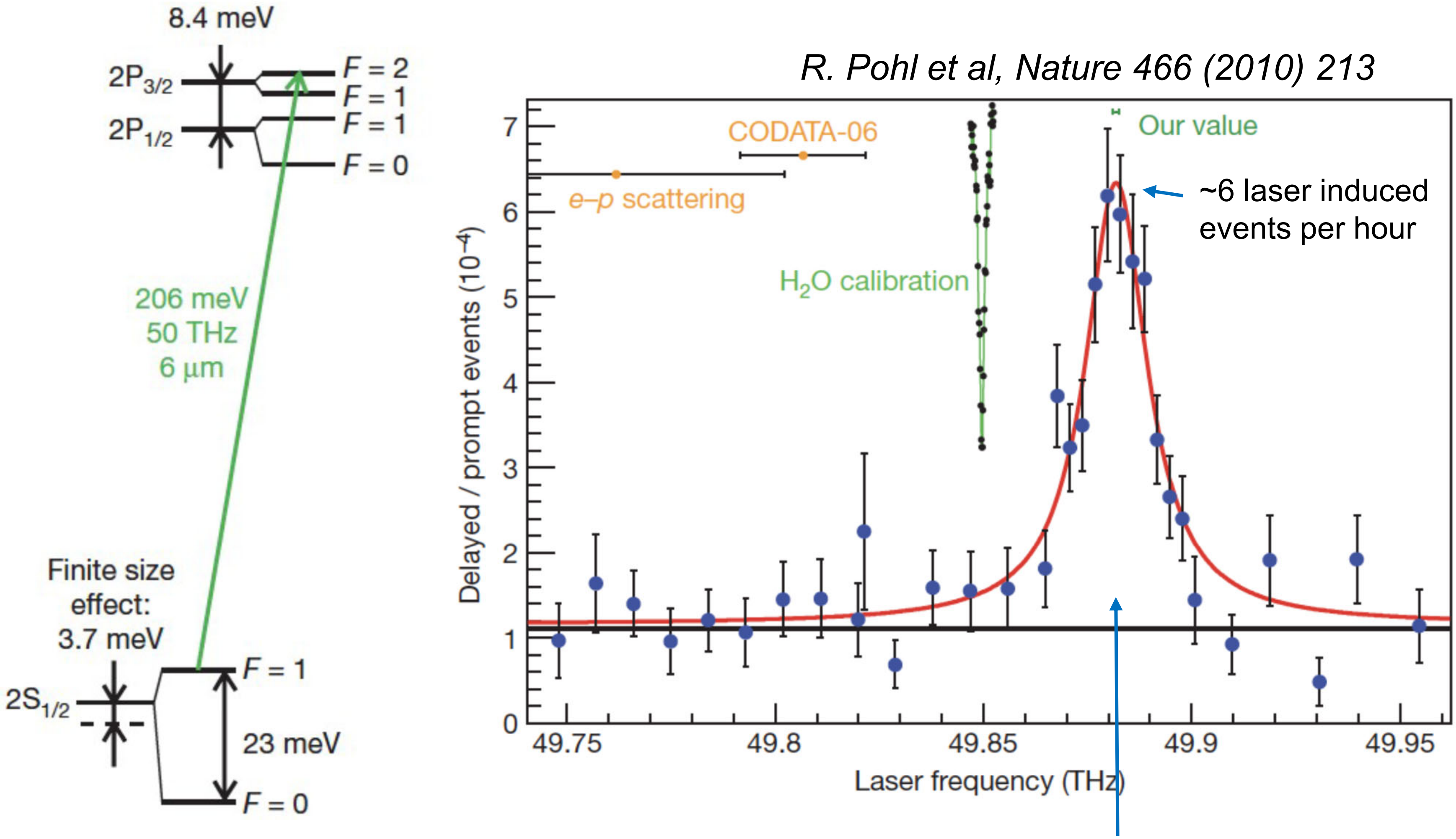

~6 laser induced events per hour

49.88188 (70) THz

r_p = 0.84184 (67) fm
much more precise, but 5σ below CODATA value of 0.8768 (69) fm

= “Proton radius puzzle”

Recent summary of the proton radius data:

https://doi.org/10.3390/universe9040182

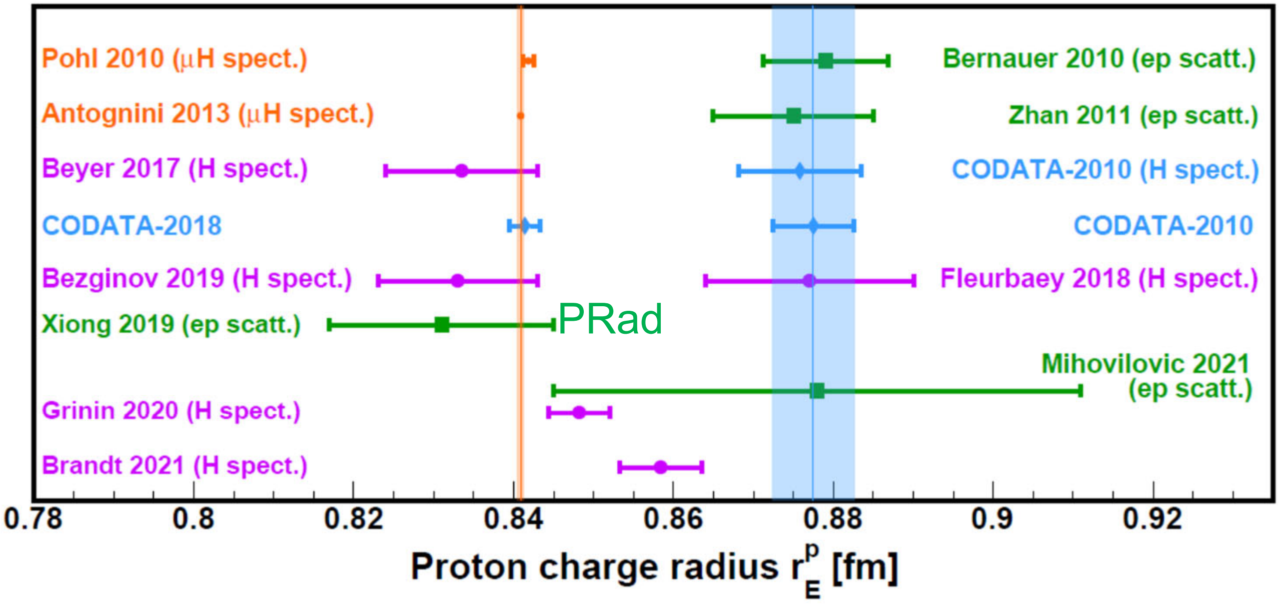

← Mainz 2010

Mainz ISR

Figure 1. The proton charge radius determined from *ep* elastic scattering, hydrogen spectroscopic experiments, as well as world-data compilation from CODATA since 2010. The muonic spectroscopic measurements [19,20] are shown in orange dots, ordinary hydrogen spectroscopic results [12–16] are shown in purple dots, electron scattering measurements [2–4,6] are shown in green squares, and blue diamonds show the CODATA compilations [18,57].

New hydrogen results since 2010: improvement from new laser techniques and better control of systematic.

New ep scattering since 2010: new Mainz measurement using ISR techniques to access lower Q^2 values; new results from PRad (Jlab, windowless target).

In addition different theoretical revisions (TPE, radiative corrections, dispersion relations to interpret FF).

→ very active field!